JOURNAL OF PROPULSION AND POWER
Vol. 24, No. 6, November–December 2008

Opportunities for a Liquid Rocket Feed System Based on Electric Pumps

N. Soldà* and D. Lentini†
University of Rome "La Sapienza," 00184 Rome, Italy

DOI: 10.2514/1.35074

A feed system for liquid-propellant rocket engines based on electric pumps powered by batteries is proposed. It is proven to stand as a viable alternative to the pressure-gas feed system. The dependence of the feed system mass on the different operating parameters is obtained so as to identify the conditions favoring its adoption, that is, a relatively long burning time and a fairly high chamber pressure. Under such conditions, the proposed system is shown to offer significant mass savings with respect to the pressure-gas system when advanced batteries are used. This advantage is further enhanced by the beneficial effect of chamber pressure on the engine effective exhaust velocity. A test case for a low Earth orbit to geostationary equatorial orbit transfer is also presented to identify the optimum value of the burning time, deriving from the competition between the feed system mass and the effect of gravitational losses.

Nomenclature

C_F	=	thrust coefficient
C_1, C_2	=	constants defined by Eqs. (12) and (13)
c	=	effective exhaust velocity
c^*	=	characteristic velocity
D_1–D_8	=	constants defined by Eqs. (31–38)
E_e	=	electric energy
f, g	=	functions defined by Eqs. (14) and (39)
$\mathcal{M}_g$	=	pressurizing gas molar mass
m	=	mass
O/F	=	oxidizer-to-fuel mass ratio
P_e	=	electric power
p	=	pressure
Q_f, Q_o	=	quantities defined by Eqs. (21) and (22)
R^0	=	universal gas constant
r	=	tank radius
T	=	absolute temperature
t_b	=	burning time
$t_{\mathrm{ba}}, t_{\mathrm{bp}}$	=	apogee and perigee burning times
V	=	volume
v	=	velocity
$\alpha, \alpha_f, \alpha_o$	=	quantities defined by Eq. (4)
γ_g	=	pressurizing gas specific heat ratio
$\Delta v_a, \Delta v_b, \Delta v_{\mathrm{tot}}$	=	apogee, perigee, and total velocity increment
δ_E, δ_P	=	battery energy and power densities
δ_t	=	density of tank wall material
η_{ep}	=	overall efficiency of electric pumps
κ_b	=	safety factor for batteries
κ_g	=	safety factor for pressurizing gas mass
$\kappa_{p1}, \kappa_{p2}, \kappa_{p3}$	=	pressure ratios defined by Eqs. (2), (16), and (17)
κ_t	=	safety factor for tank wall thickness
κ_u	=	quantity defined by Eq. (3)
λ	=	payload mass ratio
μ_{ep}	=	electric pump specific mass
ρ	=	fluid density
σ_t	=	stress admitted by tank wall material
τ	=	tank wall thickness

Subscripts

b	=	batteries
c	=	combustion chamber
ep	=	electric pumps
eps	=	electric pump system
f	=	fuel
fs	=	feed system
g	=	pressurizing gas
min	=	minimum
o	=	oxidizer
p	=	propellant
pgs	=	pressure-gas system
t	=	tank
0	=	initial conditions in pressure-gas tank

I. Introduction

CURRENT feed systems for liquid rocket engines are either turbopump fed or pressure-gas fed [1,2]. It is well known that the former ensures a lightweight design, yet with the drawbacks of mechanical complexity and the ensuing limited reliability (e.g., a large fraction of launch failures are due to malfunctioning turbopump systems), long development times, and high costs; further, restartability is limited. On the other hand, the latter system is conceptually simple and ensures unlimited restartability, but is very heavy owing to the tanks being under pressure; further, development may be lengthy, despite its apparent simplicity.

A third option based on electric feed pumps powered by batteries is proposed here. It is apparent that the bottleneck in this case is the mass of the batteries, which is dictated by the most stringent one of two requirements: 1) ensure the electrical power P_e required by the pumps, and 2) ensure the electrical energy E_e required to drive the pumps throughout their operating time t_b. Given the relatively limited power and energy density of today's batteries, it is felt that the proposed system cannot compete with a turbopump-fed system (e.g., as applied in the booster stages). However, the comparison is found to be favorable with respect to the pressure-gas system, that is, in applications to upper stages and spacecraft propulsion systems. Consequently, the comparison reported herein is restricted to just the pressure-gas and electric pump systems. Derivations aimed at identifying the mass of the feed system for both the standard pressure-gas system and the proposed system are presented in Sec. II. Then, a comparison of the two systems is given in Sec. III, including a test case of a low Earth orbit (LEO) to a geostationary equatorial

Received 10 October 2007; accepted for publication 5 July 2008.

*Research Student.
†Associate Professor, Dipartimento di Meccanica e Aeronautica, Via Eudossiana 18; diego.lentini@uniroma1.it. Senior Member AIAA.

orbit (GEO) transfer. Finally, conclusions about the possible convenience of the proposed feed system are drawn in Sec. IV.

II. Evaluation of Feed System Mass

A. Pressure-Gas System

The main components of the total mass m_{pgs} of a feed system using pressurized gas are the mass m_g of the pressurizing gas and the masses of the tanks for the gas itself, the fuel and the oxidizer, denoted as $m_{t,g}$, $m_{t,f}$, and $m_{t,o}$, respectively:

$$m_{\text{pgs}} = m_g + m_{t,g} + m_{t,f} + m_{t,o} \tag{1}$$

The mass of the plumbing is not included in Eq. (1) for m_{pgs}; however, it will certainly be greater for the system presently under consideration as compared with the system proposed herein in view of the higher pressures involved. Therefore, neglecting it stands as a conservative assumption in the comparison of the two feed concepts in Sec. III.

We consider a regulated pressure system and, for the sake of conciseness, we further assume that the pressure inside the tanks is the same for the two propellants, $p_{t,f} = p_{t,o}$ (this assumption, as well as similar ones that will be introduced next, can be easily relieved if necessary). We accordingly introduce a ratio between the propellant tank pressure and the chamber pressure:

$$\kappa_{p1} = \frac{p_{t,f}}{p_c} = \frac{p_{t,o}}{p_c} \tag{2}$$

We then introduce, to account for ullage, a ratio between the tank volume and the (initial) propellant volume, which we also assume to be the same for the two propellants:

$$\kappa_u = \frac{V_{t,f}}{V_f} = \frac{V_{t,o}}{V_o} \tag{3}$$

Further coefficients to be defined to account for design margins are a factor κ_g multiplying the pressure-gas mass strictly required, a safety factor $\kappa_{t,g}$ relating to the thickness of the wall of the pressure-gas tank, and a similar factor $\kappa_{t,p}$ for the propellant tanks (again, assumed to be the same for both propellants).

The different items at the right-hand side of Eq. (1) will now be determined. Let m_p denote the total (oxidizer plus fuel) propellant mass and O/F the oxidizer-to-fuel mass ratio. Then let γ_g and $\mathcal{M}_g$ indicate the specific heat ratio and the molar mass of the pressurizing gas, T_0 and p_0 its initial temperature and pressure, and R^0 the universal gas constant. Upon introducing the positions

$$\alpha_f = \frac{1}{\rho_f}\frac{1}{1+O/F}, \qquad \alpha_o = \frac{O/F}{\rho_o}\frac{1}{1+O/F}, \qquad \alpha = \alpha_f + \alpha_o \tag{4}$$

the required mass of the pressurizing gas can be determined after [2], when the margins defined above are taken into account, as

$$m_g = \alpha\kappa_{p1}\kappa_u\kappa_g \frac{\gamma_g \mathcal{M}_g}{R^0 T_0}\frac{m_p p_c}{1-\kappa_{p1}p_c/p_0} \tag{5}$$

As far as the tank masses are concerned, they can be expressed as the wall material density times the tank wall surface times the wall thickness. By assuming spherical tanks, the radius of the pressurizing gas tank can be related to its volume $V_{t,g}$ and then to the gas mass as

$$r_{t,g} = \left(\frac{3}{4\pi}V_{t,g}\right)^{1/3} = \left(\frac{3}{4\pi}\frac{m_g}{\rho_0}\right)^{1/3} = \left[\frac{3}{4\pi}\frac{m_g}{p_0\mathcal{M}_g/(R^0T_0)}\right]^{1/3} \tag{6}$$

where ρ_0 denotes the initial gas density. The wall thickness is given by Laplace's law, multiplied by the relevant safety factor $\kappa_{t,g}$:

$$\tau_g = \kappa_{t,g}\frac{r_{t,g}p_0}{2\sigma_{t,g}} = \frac{\kappa_{t,g}p_0}{2\sigma_{t,g}}\left[\frac{3}{4\pi}\frac{m_g}{p_0\mathcal{M}_g/(R^0T_0)}\right]^{1/3} \tag{7}$$

Here, $\sigma_{t,g}$ is the maximum stress admitted by the wall material; in particular, it refers to the yield stress for plastic materials and to the ultimate stress for fragile materials. Accordingly, the mass of the pressurizing gas tank turns out to be

$$m_{t,g} = \frac{3}{2}\alpha\kappa_{p1}\kappa_u\kappa_g\kappa_{t,g}\gamma_g\frac{\delta_{t,g}}{\sigma_{t,g}}\frac{m_p p_c}{1-\kappa_{p1}p_c/p_0} \tag{8}$$

where $\delta_{t,g}$ is the density of the wall material. Similarly, for the propellant tanks, still assumed to be spherical, it results in

$$m_{t,f} = \frac{3}{2}\alpha_f\kappa_{p1}\kappa_u\kappa_{t,p}\frac{\delta_{t,p}}{\sigma_{t,p}}m_p p_c \tag{9}$$

$$m_{t,o} = \frac{3}{2}\alpha_o\kappa_{p1}\kappa_u\kappa_{t,p}\frac{\delta_{t,p}}{\sigma_{t,p}}m_p p_c \tag{10}$$

Incidentally, nonspherical tank shapes would entail larger wall thicknesses due to stress concentrations [1]. Notice that in pressure-fed systems the tanks are thick walled. After Eq. (1), the total mass of such a system results in

$$m_{\text{pgs}} = \left\{\left[\gamma_g\left(\frac{\mathcal{M}_g}{R^0T_0} + \frac{3}{2}\kappa_{t,g}\frac{\delta_{t,g}}{\sigma_{t,g}}\right)\kappa_g\right]\frac{1}{1-\kappa_{p1}p_c/p_0} + \frac{3}{2}\kappa_{t,p}\frac{\delta_{t,p}}{\sigma_{t,p}}\right\}\alpha\kappa_{p1}\kappa_u m_p p_c \tag{11}$$

Such an expression can be put in a more synthetic form by defining the constants:

$$C_1 = \gamma_g\left(\frac{\mathcal{M}_g}{R^0T_0} + \frac{3}{2}\kappa_{t,g}\frac{\delta_{t,g}}{\sigma_{t,g}}\right)\alpha\kappa_g\kappa_{p1}\kappa_u \tag{12}$$

$$C_2 = \frac{3}{2}\alpha\kappa_{t,p}\kappa_{p1}\kappa_u\frac{\delta_{t,p}}{\sigma_{t,p}} \tag{13}$$

which allow, in particular, the recasting of the expression of the ratio of m_{pgs} to the propellant mass in the following form:

$$\frac{m_{\text{pgs}}}{m_p} = \left(\frac{C_1}{1-\kappa_{p1}p_c/p_0} + C_2\right)p_c = f(p_c, p_0) \tag{14}$$

with emphasis on the arguments.

B. Electric Pump System

The main components of the total mass m_{eps} of the proposed feed system based on electric pumps are, again, a (small) pressurizing gas mass required to avoid cavitation, the masses of the tanks for the gas itself, the fuel and the oxidizer, plus the masses m_{ep} and m_b of the electric pumps (here taken inclusive of the power conditioning/controller unit mass) and the batteries, respectively:

$$m_{\text{eps}} = m_g + m_{t,g} + m_{t,f} + m_{t,o} + m_{\text{ep}} + m_b \tag{15}$$

We again assume that the ratio, here denoted as κ_{p2} (obviously, $\kappa_{p2} \ll \kappa_{p1}$), between the pressure in the tanks and in the chamber is the same for both propellants:

$$\kappa_{p2} = \frac{p_{t,f}}{p_c} = \frac{p_{t,o}}{p_c} \tag{16}$$

and further that the pressure rise provided by the pumps is also the same for both propellants, so that a ratio

$$\kappa_{p3} = \frac{\Delta p_f}{p_c} = \frac{\Delta p_o}{p_c} \tag{17}$$

can be defined. Actually, if one of the propellants is used for regenerative cooling (usually fuel), it must undergo a higher pressure

rise to compensate for losses in the cooling channels; this can be easily accommodated in the formulation if necessary, but at this stage it is not considered an essential point. The masses of the various entries of Eq. (15) will now be derived. For m_g and $m_{t,g}$, expressions analogous to Eqs. (5) and (8) hold, but with κ_{p2} in place of κ_{p1}. As far as the propellant tanks are concerned, the wall thickness required is, in principle, again given by Laplace's law, for example, for fuel and oxidizer, respectively,

$$\tau_f = \frac{\kappa_{p2}\kappa_{t,p}}{2\sigma_{t,p}} p_c \left(\frac{3\kappa_u \alpha_f}{4\pi} m_p\right)^{1/3} \tag{18}$$

$$\tau_o = \frac{\kappa_{p2}\kappa_{t,p}}{2\sigma_{t,p}} p_c \left(\frac{3\kappa_u \alpha_o}{4\pi} m_p\right)^{1/3} \tag{19}$$

However, in the case of pump feeding, the tanks are thin walled, and the thickness as defined by Eqs. (18) and (19), may turn out to be too small to withstand acceleration loads. To account for this circumstance, a minimum thickness $\tau_{\min}$ is introduced; it can be easily seen that the condition that causes the wall thickness to stick at this limit is

$$p_c m_p^{1/3} < Q_f \text{ for fuel}, \qquad p_c m_p^{1/3} < Q_o \text{ for oxidizer} \tag{20}$$

where

$$Q_f = \frac{2\sigma_{t,p}\tau_{\min}}{\kappa_{p2}\kappa_{t,p}} \left(\frac{4\pi}{3\kappa_u \alpha_f}\right)^{1/3} \tag{21}$$

$$Q_o = \frac{2\sigma_{t,p}\tau_{\min}}{\kappa_{p2}\kappa_{t,p}} \left(\frac{4\pi}{3\kappa_u \alpha_o}\right)^{1/3} \tag{22}$$

Accordingly, if $p_c m_p^{1/3} > Q_f$, then the fuel tank mass is

$$m_{t,f} = \frac{3}{2}\alpha_f \kappa_{p2}\kappa_u \kappa_{t,p} \frac{\delta_{t,p}}{\sigma_{t,p}} m_p p_c \tag{23}$$

and if $p_c m_p^{1/3} > Q_o$, then the oxidizer tank mass is

$$m_{t,o} = \frac{3}{2}\alpha_o \kappa_{p2}\kappa_u \kappa_{t,p} \frac{\delta_{t,p}}{\sigma_{t,p}} m_p p_c \tag{24}$$

However, in the event that $p_c m_p^{1/3} < Q_f$ and/or $p_c m_p^{1/3} < Q_o$, the relevant tank masses are determined as

$$m_{t,f} = (4\pi)^{1/3}(3\kappa_u \alpha_f)^{2/3}\tau_{\min}\delta_{t,p} m_p^{2/3} \tag{25}$$

$$m_{t,o} = (4\pi)^{1/3}(3\kappa_u \alpha_o)^{2/3}\tau_{\min}\delta_{t,p} m_p^{2/3} \tag{26}$$

The definition of the masses of the electric pumps and the batteries is now considered. The electric energy required over the whole engine operating time t_b is

$$E_e = \frac{\alpha\kappa_{p3}}{\eta_{\text{ep}}} m_p p_c \tag{27}$$

where η_{ep} is the overall efficiency of the conditioning/controller and electric pump unit, and the power is obviously

$$P_e = (E_e/t_b) \tag{28}$$

Accordingly, the mass of the electric pumps can be determined in terms of their specific mass μ_{ep} (mass per unit electric power absorbed):

$$m_{\text{ep}} = \mu_{\text{ep}} P_e = \mu_{\text{ep}}(E_e/t_b) \tag{29}$$

As far as the batteries are concerned, their mass depends on whether the constraint on the power or the energy is more stringent:

$$m_b = \kappa_b \max\left(\frac{P_e}{\delta_P}, \frac{E_e}{\delta_E}\right) \tag{30}$$

where a factor κ_b is introduced to account for the design margins. We further introduce the following constants:

$$D_1 = \gamma_g \left(\frac{\mathcal{M}_g}{R^0 T_0} + \frac{3}{2}\kappa_{t,g}\frac{\delta_{t,g}}{\sigma_{t,g}}\right)\alpha\kappa_g\kappa_{p1}\kappa_u \tag{31}$$

$$D_2 = \frac{3}{2}\alpha_f \kappa_{t,p}\kappa_{p2}\kappa_u \frac{\delta_{t,p}}{\sigma_{t,p}} \tag{32}$$

$$D_3 = (4\pi)^{1/3}(3\kappa_u \alpha_f)^{2/3}\tau_{\min}\delta_{t,p} \tag{33}$$

$$D_4 = \frac{3}{2}\alpha_o \kappa_{t,p}\kappa_{p2}\kappa_u \frac{\delta_{t,p}}{\sigma_{t,p}} \tag{34}$$

$$D_5 = (4\pi)^{1/3}(3\kappa_u \alpha_o)^{2/3}\tau_{\min}\delta_{t,p} \tag{35}$$

$$D_6 = \frac{\alpha\kappa_{p3}\mu_{\text{ep}}}{\eta_{\text{ep}}} \tag{36}$$

$$D_7 = \frac{\alpha\kappa_b\kappa_{p3}}{\eta_{\text{ep}}\delta_P} \tag{37}$$

$$D_8 = \frac{\alpha\kappa_b\kappa_{p3}}{\eta_{\text{ep}}\delta_E} \tag{38}$$

After Eq. (15), the ratio of the total mass of the electric pump system to the propellant mass can be put in the following form:

$$\begin{aligned}\frac{m_{\text{eps}}}{m_p} &= \frac{D_1}{1-\kappa_{p2}p_c/p_0} p_c + \max\left(D_2 p_c, \frac{D_3}{m_p^{1/3}}\right) \\ &\quad + \max\left(D_4 p_c, \frac{D_5}{m_p^{1/3}}\right) + D_6\frac{p_c}{t_b} + \max\left(\frac{D_7 p_c}{t_b}, D_8 p_c\right) \\ &= g(p_c, p_0, m_p, t_b)\end{aligned} \tag{39}$$

III. Comparison of the Two Systems

As already indicated, the mass of the batteries in the proposed system depends on either the energy or the power requirements, according to which is the most stringent. For a given battery, the values of the power density δ_P and the energy density δ_E depend on the discharge time, which in the present context is the engine burning time t_b; such a relationship is given by Ragone's plot [3,4]. Figure 1 shows such a plot for commercially available, premium Li-polymer batteries,[‡] which are representative of the best technology currently available. Notice that the line interpolating the data is limited to a minimum discharge time of about 12.5 min; accordingly, this is the minimum burning time considered in the comparison. It is also important to note that the choice of energy storage device is not limited to batteries, but might also include supercapacitors and fuel cells. However, the former suffer from limited energy density

[‡]Data available online at www.symmetryresourcesinc.com [retrieved on 26 August 2008].

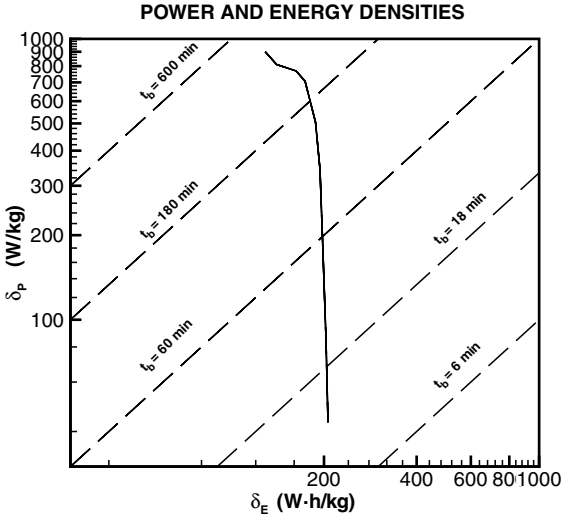

Fig. 1 Ragone plot of premium Li-polymer batteries.

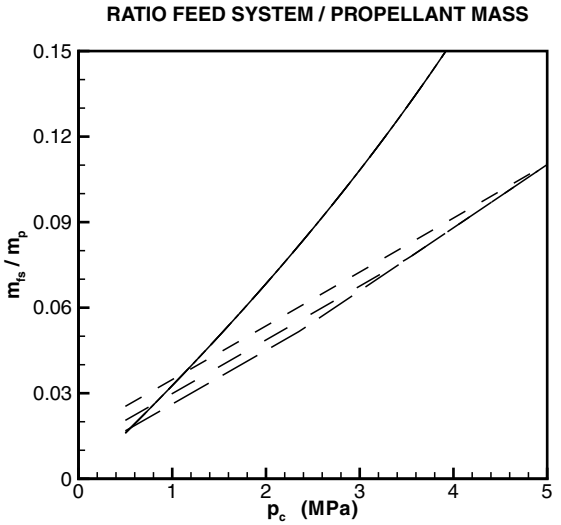

Fig. 2 Ratio of feed system mass over total propellant mass as a function of chamber pressure for $p_0 = 20$ MPa and $t_b = 1000$ s. Solid line: pressure-gas system; dashed line: proposed system $m_p = 1000$ kg; long-dashed line: $m_p = 3000$ kg; and extra-long-dashed line: $m_p = 10,000$ kg.

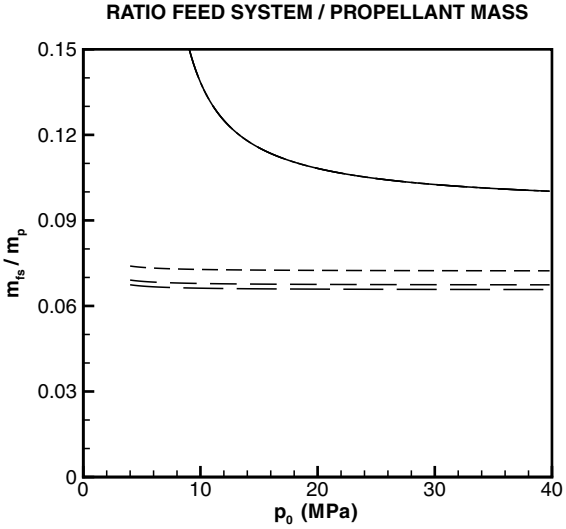

Fig. 3 Ratio of feed system mass over total propellant mass as a function of initial helium pressure for $p_c = 3$ MPa and $t_b = 1000$ s. Solid line: pressure-gas system; dashed line: proposed system $m_p = 1000$ kg; long-dashed line: $m_p = 3000$ kg; and extra-long-dashed line: $m_p = 10,000$ kg.

whereas the latter, despite giving a performance even higher than batteries on a mass basis, result in a much lower volumetric performance, unless the reactant storage pressure is assumed to be greater than about 60 MPa [5],[§] which is about 20 times as much as current technology cells. Further, fuel cells require the handling of cryogenic reactants (oxygen and hydrogen), which can be inconvenient for small upper stages and spacecraft.

Quite obviously, the preference for one system or the other (turbopumps or electric pumps) depends to a critical extent on the values of several performance parameters absorbed in the constants C_1, C_2, and D_1–D_8. To work out a comparison of the two systems, we consider a nitrogen tetroxide/monomethylhydrazine (NTO/MMH) propellant combination in a ratio that will ensure equal volume tanks. Further, we assume helium as the pressurant gas, stored at ambient temperature. As far as the tank material is concerned, Kevlar® is chosen for the pressurant gas tank, whereas aluminum alloy is assumed for the propellant tanks. Accordingly, the following values are assumed in the present calculations:

$\kappa_{p1} = 1.8$	$\kappa_{p2} = 0.3$	$\kappa_{p3} = 1.5$
$\kappa_g = 1.3$	$\kappa_{t,g} = 2.4$	$\kappa_{t,p} = 1.25$
$\kappa_u = 1.05$	$\kappa_b = 1.2$	$\tau_{\min} = 1$ mm
$\gamma_g = 1.667$	$\mathcal{M}_g = 4.0026$ kg/kmol	$T_0 = 288.15$ K
$\rho_o = 1431$ kg/m^3	$\rho_f = 874$ kg/m^3	$O/F = \rho_o/\rho_f$
$\delta_{t,g} = 1700$ kg/m^3	$\delta_{t,p} = 2800$ kg/m^3	
$\sigma_{t,g} = 3300$ MPa	$\sigma_{t,p} = 455$ MPa	
$\eta_{\text{ep}} = 0.68$	$\mu_{\text{ep}} = 6$ kg/kW$_e$	

Notice that the values assumed for the parameters are quite conservative, aimed at avoiding a bias toward one particular feed system.

As seen in Eq. (14), the mass of a pressure-gas feed system, divided by the overall propellant mass, depends on the chamber pressure p_c and the initial gas pressure p_0. The mass of the proposed system based on electric pumps (39) also depends on p_c and p_0 and, in addition, on the burning time and the propellant mass itself in the case that the tank thickness is dictated by the constraint not to be smaller than a given value $\tau_{\min}$. We will therefore first examine the trend of the ratio between the feed system mass m_{fs} and the propellant mass m_p as a function of the chamber pressure for a value of p_0 set to 20 MPa (see also the comment on Fig. 3 in the next paragraph), a burning time set to 2000 s, and for three values of the propellant mass, 1000, 3000, and 10,000 kg. Such trends are shown in Fig. 2 for the two feed systems under consideration. The curves for the electric pump system, referring to the aforementioned values of m_p, exhibit a separate, nearly parallel, trend for relatively low values of p_c, indicating that the factor limiting the wall thickness is the constraint $\tau \geq \tau_{\min}$. However, for chamber pressures slightly above 3.5 MPa, the curves for $m_p = 3000$ and 10,000 kg coalesce into a single curve, as under such circumstances the wall thickness is greater than $\tau_{\min}$, so that the walls are actually sized according to Laplace's law. The figure further suggests that, for p_c greater than about 5 MPa, the curve for $m_p = 1000$ kg will also coalesce with the others. It is worth noting that the separate trends for the three curves follow from the assumption of the same minimum thickness for the three values of m_p under consideration; if the minimum thickness is instead assumed to be proportional to the cubic root of m_p, the variable m_p is dropped from the arguments of function g in Eq. (39). In summation, Fig. 2 indicates that the proposed feed system is preferable when the chamber pressure is above roughly 1 MPa.

[§]Data available online at gltrs.grc.nasa.gov [retrieved on 26 August 2008].

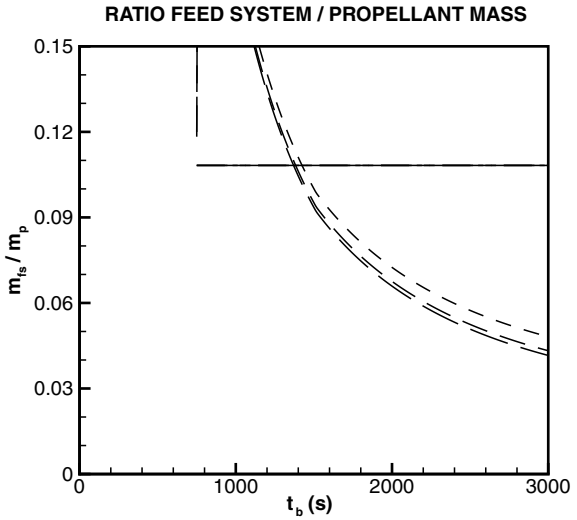

Fig. 4 Ratio of feed system mass over total propellant mass as a function of burning time for $p_c = 3$ MPa and $p_0 = 20$ MPa. Solid line: pressure-gas system; dashed line: proposed system $m_p = 1000$ kg; long-dashed line: $m_p = 3000$ kg; and extra-long-dashed line: $m_p = 10,000$ kg.

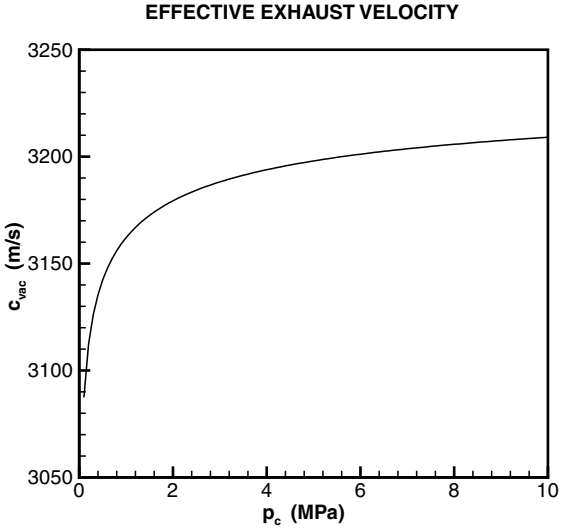

Fig. 5 Theoretical effective exhaust velocity of an isovolumetric NTO/MMH propellant combination as a function of chamber pressure.

Figure 3 shows the effect of the initial gas pressure p_0 on the ratio $m_{\rm fs}/m_p$ for the two feed systems and the three values of m_p being considered for a chamber pressure set at 3 MPa and the same burning time as already mentioned. It is seen that, for the pressure-gas system, a high initial pressure is desirable; however, the advantage becomes marginal over 20–25 MPa. For the proposed system, p_0 turns out to be rather inconsequential, as the pressurization is limited to the small amount required to avoid pump cavitation.

The effect of the burning time (for $p_c = 3$ MPa and $p_0 = 20$ MPa) on the ratio $m_{\rm fs}/m_p$ is depicted in Fig. 4. The range of burning times is bound by the minimum discharge time for the batteries at hand, which can be estimated from Fig. 1 to be about 750 s, whereas the upper value is set to 3000 s because relatively little advantage is obtained by further prolonging the duration of the burn. Notice that, in the case of multiple engine ignitions, here t_b has the meaning of the cumulative burning time. It is clearly visible that, although t_b does not affect $m_{\rm fs}/m_p$ for the pressure-gas system, it does have the effect of reducing the relative feed system mass for the proposed system. In fact, once the propellant mass is assigned, a longer burning time implies a reduced propellant mass flow rate, that is, a reduced power (and then mass) of the electric pumps, and possibly of the batteries, if their mass is power constrained (see also Fig. 9).

As mentioned with reference to Fig. 2, a quantity critical to assessing the advantage of the proposed system over the pressure-gas one is the chamber pressure, with high values of p_c favoring the proposed system, which is an obvious consequence of the tanks not being under pressure. Such a system would then be particularly valuable for high-chamber-pressure engines, which exhibit the additional advantage of a larger effective exhaust velocity (i.e., specific impulse). Indeed, both the thrust coefficient C_F and the characteristic velocity c^* increase with increasing pressure. Figure 5 illustrates the trend of the ideal effective exhaust velocity (in a vacuum, for a nozzle expansion ratio of 40) $c_{\rm vac} = C_F c^*$ as a function of chamber pressure for a similar test case using an isovolumetric NTO/MMH propellant combination, as computed via the equilibrium chemical solver CEA [6,7][¶]; to take some account of finite rate chemistry, the flow is assumed to suddenly freeze at the throat, although, more precisely, the impact of finite rate chemistry depends on the nozzle size [8]. Accordingly, the gain in effective exhaust velocity adds up to that of a reduced feed system mass, with an ensuing beneficial effect on the payload mass.

[¶]Code available online at www.grc.nasa.gov [retrieved on 26 August 2008].

To further quantify the advantage associated with the proposed system, an example is presented of the case of a propulsion system tailored for a Hohmann transfer, that is, one aimed at injecting a payload initially in an equatorial LEO with a 300-km-altitude into a geostationary transfer orbit (GTO), and then circularizing the latter into a GEO. The ideal (i.e., referring to an impulse maneuver) velocity increment requirements are 2426 m/s for the perigee kick and 1466 m/s for the apogee burn. For a finite time perigee burn, the Δv requirements increase due to gravitational losses. This effect is estimated here via a computational code based on assumptions adequate for the present level of analysis (tangential thrusting, spherical Earth, neglect of aerodynamic drag effects, neglect of the influence of third bodies, etc.), and the results are shown in Fig. 6, based on an assumed value of the (real) effective exhaust velocity of 3000 m/s, as appropriate to the NTO/MMH propulsion system outlined earlier (gravitational losses weakly depend on the effective exhaust velocity). It is seen that the perigee velocity increment Δv_p increases with the duration of the perigee burn $t_{\rm bp}$; however, the value of the required apogee velocity increment Δv_a decreases, because longer perigee burning times result in GTOs of smaller eccentricity. Notice that, in Fig. 6, the Δv_a are computed by neglecting apogee gravitational losses, an assumption justified in view of the very high

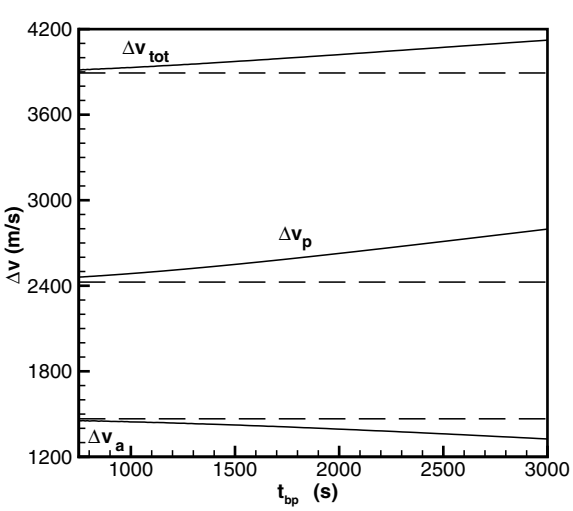

Fig. 6 Velocity increments required for the perigee and apogee maneuvers of a transfer between a 300-km-altitude LEO and GEO, and total Δv, as a function of perigee burning time (assuming $c = 3000$ m/s).

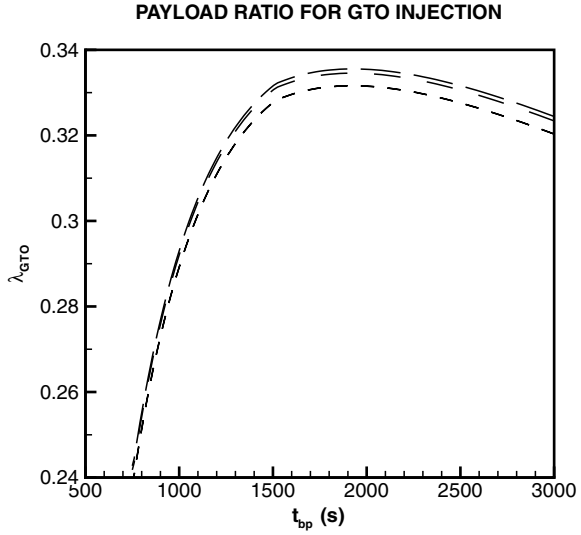

Fig. 7 Payload ratio for injection into GTO as a function of perigee burning time (assuming $c = 3000$ m/s) with the proposed feed system. Dashed line: $m_p = 1000$ kg; long-dashed line: $m_p = 3000$ kg; and extra-long-dashed line: $m_p = 10,000$ kg.

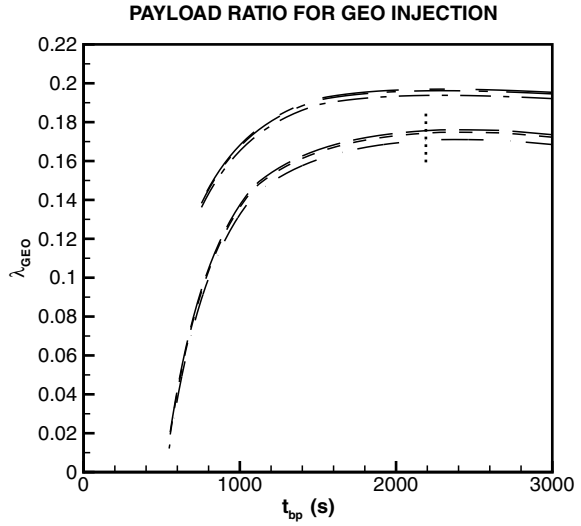

Fig. 8 Payload ratio for injection into GEO as a function of perigee burning time (assuming $c = 3000$ m/s) with the proposed feed system. Single-stage option—dashed line: $m_p = 1000$ kg; long-dashed line: $m_p = 3000$ kg; and extra-long-dashed line: $m_p = 10,000$ kg; two-stage option— dashed-dotted line: $m_p = 1000$ kg; long-dashed-dotted line: $m_p = 3000$ kg; and extra-long-dashed-dotted line: $m_p = 10,000$ kg.

altitude of the GEO. However, the two opposing trends do not cancel out, resulting in a $\Delta v_{\text{tot}} = \Delta v_p + \Delta v_a$ still mildly increasing with t_{bp}. In the following paragraphs, the effect of the perigee burning time on two payload ratios, one referring to the first phase of the maneuver, accordingly defined as

$$\lambda_{\text{GTO}} = \frac{m_{\text{GTO}}}{m_{\text{LEO}}} \tag{40}$$

and a second referring to the whole transfer

$$\lambda_{\text{GEO}} = \frac{m_{\text{GEO}}}{m_{\text{LEO}}} \tag{41}$$

is evaluated. Here m_{LEO} is the initial mass in LEO, whereas m_{GTO} and m_{GEO} clearly stand for the payload mass in the respective orbits. The former payload ratio is shown in Fig. 7 as a function of the perigee burning time. The payload ratio considered in Fig. 7 and the figures that follow is recovered by including in the stage structural mass the feed system mass as detailed earlier and an extra mass indicatively made equal to 4% of the propellant plus pressurant mass to account for other structures. Further, a 3% propellant margin is assumed. Two effects contribute to the determination of the shape of the curve: the reduction of the feed system mass with the burning time already assessed in Fig. 4 (resulting in a larger payload), and the increase of the effective Δv_p with t_{bp}. Their combined effect determines a maximum around a perigee burning time of 1900 s. Such a maximum spans a narrow range (from about 0.3316 to 0.3355) depending on the assumed propellant mass.

To arrive at the overall payload ratio λ_{GEO} for the whole transfer, two propulsive options are considered: 1) a single-stage, restartable system, performing both the perigee and the apogee burns; and 2) a two-stage system (one to be fired near the perigee, the other near the apogee of the GTO) with independent engines. Both options are assumed to be fed via the proposed system. Results are shown in Fig. 8 for both options. In the single-stage option (dashed lines), the overall burning time t_b is split between the time taken by the perigee burn t_{bp} and that referring to the apogee burn t_{ba}; because of the aforementioned limitations in the discharge rate of the batteries under consideration, the cumulative burning time $t_{\text{bp}} + t_{\text{ba}}$ must be greater than 750 s (unless oversizing the batteries) and less than 3000 s. However, no constraint applies as far as the split of the total burning time t_b over the burns. It follows that t_{bp} can, in principle, span the whole range of 0–3000 s (although small values will result in high accelerations and, in addition, heavy thrusters). However, in the present case, it is found that perigee burning times shorter than about

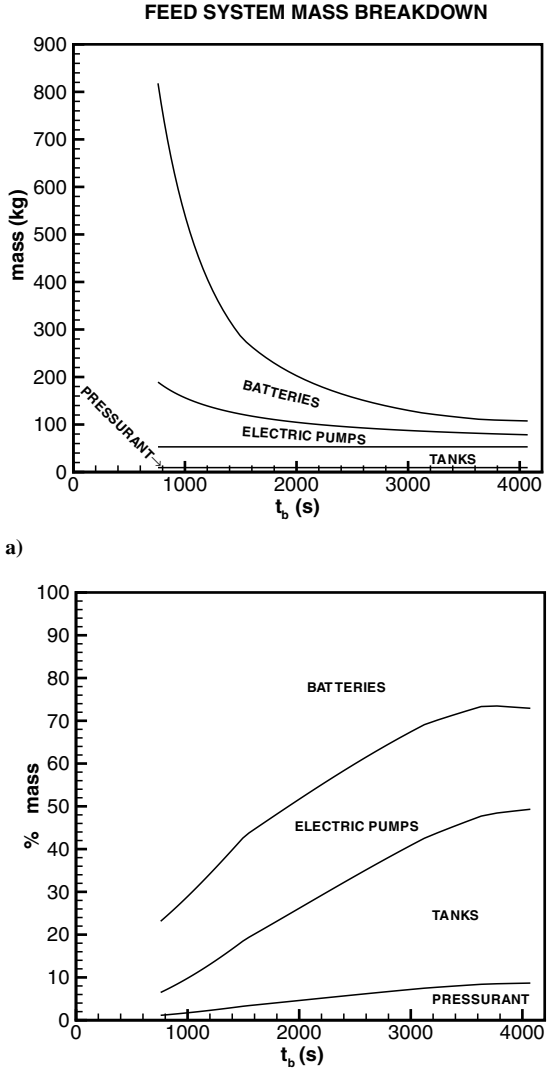

Fig. 9 Mass breakdown of the electric pump feed system for single-stage injection into LEO (assuming $m_p = 3000$ kg and $c = 3000$ m/s): a) absolute terms, and b) percentage terms.

550 s (corresponding to a total perigee-plus-apogee burning time of about 750 s) result in a zero payload ratio, due to an excessive feed system mass for short burning times (see also the comment on Fig. 9 below). Notice that, for t_{bp} longer than about 2190 s (indicated by the dotted line in Fig. 8), the overall burning time t_b exceeds the limit of 3000 s, which, at any rate, has been chosen merely to identify a burning-time range and does not imply any physical bound. The maximum payload ratio is obtained for a perigee burning time of around 2400 s and spans the narrow range of 0.171–0.176 as the total propellant mass (burnt in the two kicks) ranges from 1000 to 10,000 kg.

In the two-stage option (dashed-dotted lines), both t_{bp} and t_{ba} contribute in principle to determining the overall payload ratio. However, because the apogee kick gravitational losses are assumed to be negligible (at least for burning times limited to a maximum of 3000 s) and, accordingly, the Δv_a to be provided by the second stage is held fixed, it is apparent that it is convenient to choose as long a t_{ba} as possible (i.e., 3000 s under the present assumptions), as this minimizes the feed system mass (see Fig. 4). Accordingly, only t_{bp}, that is, the burning time of the first stage, remains as a free parameter (in this case limited to a minimum of 750 s because of the aforementioned limit in the discharge rate of the batteries). Because the payload ratio of the second stage is roughly fixed (having fixed the Δv_a required and the burning time, it spans the range of 0.568–0.602 depending on the propellant mass of the second stage, which in turn depends on t_{bp} and the propellant mass of the first stage, as inferred by Fig. 7), the trend of the relevant curves in Fig. 8 follow that of the GTO payload ratio given in Fig. 7 (notice the different scale of the two figures). The maximum values of the payload are obtained for burning times around 2300 s and span the range of 0.194–0.197 as the propellant mass of the first stage ranges from 1000 to 10,000 kg. Accordingly, the two-stage option ensures a limited advantage with respect to the single-stage one on the order of 12–13% on a relative basis, which has to be weighted against the accompanying increase in complexity and cost, and the reduced reliability.

Finally, a mass breakdown of the electric pump system is shown in Fig. 9 for the case of the single-stage LEO to GEO transfer with a propellant mass of 3000 kg. In this case, results are plotted as a function of the overall burning time (perigee plus apogee) to highlight the impact of the cumulative burning time. The masses of the pressurant gas and of the tanks (for the propellant and pressurant) are fixed at 9.3 and 43.7 kg, respectively, for a total of 53 kg. The electric pump mass decreases from 136 to 25 kg as the burning time spans the range of 750–4070 s (which, incidentally, corresponds to the aforementioned range of perigee burning time of 548–3000 s), consistent with Eq. (29). The mass of the batteries also decreases from 629 to as few as 29 kg in the same overall burning-time range. This striking result is due to the fact that, up to a total burning time of about 3700 s, the battery mass turns out to be power constrained, so that, in view of Eqs. (27), (28), and (30), it results in

$$m_b = \frac{\alpha \kappa_b \kappa_{p3}}{\eta_{ep}} \frac{m_p p_c}{\delta_P t_b} \tag{42}$$

The first term is a constant, whereas the denominator of the second term features, in addition to a direct dependence upon the overall burning time, an indirect dependence through the power density δ_P, which is seen from the Ragone plot in Fig. 1 to greatly increase with discharge time. This further emphasizes that the proposed system is particularly advantageous for long burning times. However, for a t_b greater than about 3700 s, the battery mass becomes energy constrained, resulting in the following expression:

$$m_b = \frac{\alpha \kappa_b \kappa_{p3}}{\eta_{ep}} \frac{m_p p_c}{\delta_E} \tag{43}$$

where the only dependence on the burning time stems from the energy density. It can be seen from Fig. 1 that δ_E actually slightly decreases as the burning time increases (leading to a somewhat higher battery mass), but the effect becomes appreciable only for burning times exceeding a few hours. The mass breakdown is reported in percentage terms in Fig. 9b, indicating that, although the battery mass is the dominating item for relatively short burning times, it plays a less crucial role for the long values of the burning time as advocated.

IV. Conclusions

The plots worked out indicate that there is an interesting field of application, typified by relatively high chamber pressures and burning times, for a feed system for liquid-propellant rockets based on the use of electric pumps powered by batteries. Although the proposed system cannot compete with more complex turbopump systems for high-performance boosters, it nonetheless represents a viable alternative to pressure-fed systems; it presents an advantage not only in terms of the feed system mass, but also of the higher effective exhaust velocity that can be attained by raising the level of the chamber pressure, an option inapplicable to pressure-fed systems. Like the pressure-gas system, the proposed system ensures extended restartability (basically limited solely by battery life, which, however, is on the order of several years). It is also expected that the weaker coupling between the feed system and the chamber may alleviate combustion instabilities. Further, if secondary (i.e., rechargeable, albeit with a lower performance) cells, rather than primary cells as assumed in the present study, are used, the battery mass can be accounted for as payload mass in missions requiring extensive energy storage, such as in the case of a lunar surface probe (owing to the lengthy lunar night).

References

[1] Humble, R. W., Lewis, D., and Sackheim, R., "Liquid Rocket Propulsion Systems," *Space Propulsion Analysis and Design*, edited by R. W. Humble, G. N. Henry, and W. J. Larson, McGraw–Hill, New York, 1995.

[2] Sutton, G. P., and Biblarz, O., *Rocket Propulsion Elements*, 7th ed., Wiley, New York, 2001, pp. 203–226.

[3] Bockris, J. O'M., and Reddy, A. K. N., *Modern Electrochemistry 2B*, 2nd ed., Kluwer/Plenum, New York, 2000, p. 1856.

[4] Christen, T., and Carlen, M. W., "Theory of Ragone Plots," *Journal of Power Sources*, Vol. 91, No. 2, 2000, pp. 210–216. doi:10.1016/S0378-7753(00)00474-2

[5] Burke, K. A., "Fuel Cells for Space Science Applications," NASA TM-2003-212730, 2003; also AIAA Paper 2003-5938, 2003.

[6] Gordon, S., and McBride, B., "Computer Program for Calculation of Complex Chemical Equilibrium Compositions and Applications—I. Analysis," NASA RP 1311-I, 1994.

[7] McBride, B., and Gordon, S., "Computer Program for Calculation of Complex Chemical Equilibrium Compositions and Applications—II. Users Manual and Program Description," NASA RP 1311-II, 1996.

[8] Lentini, D., "Identification of Chemical and Vibrational Relaxation Regimes in Rocket Nozzle Flow via a Quasi-Linear Formulation," *Proceedings of the Institution of Mechanical Engineers. Part G, Journal of Aerospace Engineering*, Vol. 215, No. 2, 2001, pp. 79–87. doi:10.1243/0954410011531781

D. Talley
Associate Editor